Dynamics and distribution of doped holes in the CuO$_2$ plane of slightly doped Y$_{1-y}$Ca$_y$Ba$_2$Cu$_3$O$_6$ studied by Cu(1) NQR

A. V. Savinkov,[1] A. V. Dooglav,[1] H. Alloul,[2] P. Mendels,[2] J. Bobroff,[2] G. Collin,[2] and N. Blanchard[2]

[1]*Laboratory of Magnetic Resonance, Kazan State University, Kazan 420008, Russia*
[2]*Laboratoire de Physique des Solides, Université Paris-Sud, UMR 8502, F-91405 Orsay, France*

Cu(1) nuclear quadrupole resonance (NQR) in slightly doped YBCO$_6$:Ca compounds allows us to study the incidence of doped holes on the antiferromagnetic state. Distributions of transverse ($1/T_2$) and longitudinal ($1/T_1$) relaxation rates of the NQR are found at low temperature, which allows us to determine a fraction of doped holes which are localized. We conclude that the holes doped in the CuO$_2$ plane by Ca$^{2+} \rightarrow$Y^{3+} substitution are distributed homogeneously in the CuO$_2$ plane above 70 K and move freely in the plane. We establish that the reduction in hole mobility from metallic to variable-range hopping induces the differentiation of Cu(1) nuclei. At lower T the holes' motion slows down and we estimate that the holes localize finally in restricted regions (4–6 lattice constants) in the Coulomb potential of the Ca^{2+} ions.

PACS number(s): 74.72.Bk, 74.62.Dh, 74.25.Ha, 74.25.Jb

I. INTRODUCTION

It is known that the undoped high-temperature superconductor (HTSC)-parent compounds La$_2$CuO$_4$ and YBa$_2$Cu$_3$O$_6$ are insulators and exhibit long-range three-dimensional (3D) antiferromagnetic (AF) order, which is rapidly destroyed as holes are doped into the CuO$_2$ planes. Superconductivity occurs beyond a critical hole content of $p_h \approx 0.05 - 0.06$, where p_h is the number of doped holes per Cu atom in the CuO$_2$ plane. However it is still not clear what happens when a dilute concentration of holes is introduced into the quasi-two-dimensional (quasi-2D) antiferromagnetic background of the CuO$_2$ plane of the cuprates.

Many experiments show the occurrence at low temperature of magnetic-disordered states of the Cu^{2+} spin system in underdoped La$_{2-x}$Sr$_x$CuO$_4$. This behavior is explained by freezing of spin degrees of freedom associated with the doped holes.[1,2] Such a low-temperature magnetic disorder coexists with long-range AF order at $0 \leq p_h \leq 0.02$ (Refs. 1 and 3) and with superconductivity at $0.05 < p_h < 0.1$.[4–6] Although in these two parts of the phase diagram the corresponding disordered states are quite different, the disordered states have usually been qualified shortly as "spin-glass" states. At hole content $0.02 \leq p_h < 0.1$ short-range AF correlations take place in the CuO$_2$ plane. Most studies reveal inhomogeneous distribution of the doped holes in the plane in underdoped regimes both for $0 \leq p_h \leq 0.02$ and $0.02 \leq p_h < 0.1$ (in the latter case called sometimes "cluster spin glass"), but there is no agreement about the origin of the inhomogeneity. Some of the studies suggest that at low doping the holes are self-organized in ensembles called "stripes," i.e., hole-rich "rivers" separated by antiferromagnetic boundaries (see, for example, Refs. 7–12). Others consider the trapping potential of the dopant, defects, and disorder as sources of the inhomogeneity.[2,13–16]

Most data about the low-temperature spin-glass state and behavior of holes in the slightly doped CuO$_2$ plane were obtained for the La$_{2-x}$Sr$_x$CuO$_4$ compound, but until now there are few reports about those for highly underdoped YBa$_2$Cu$_3$O$_{6+x}$. For this system, the regime of low doping is

not readily accessible since the hole transfer from the CuO$_x$ chains to the CuO$_2$ planes is rather complex and depends critically on oxygen ordering and content. Since the chains of Y$_{1-y}$Ca$_y$Ba$_2$Cu$_3$O$_6$ are unoccupied by oxygen, p_h can be adjusted in a controlled way through the heterovalent substitution of Ca$^{2+} \rightarrow$Y^{3+}.[17] The muon spin rotation (μSR) experiments show a coexistence of the low-temperature spin-glass state and the long-range AF order at $0 \leq p_h \leq 0.035$,[4] as compared to La$_{2-x}$Sr$_x$CuO$_4$ where the AF order and the spin glass coexist at $0 \leq p_h \leq 0.02$.[1,3] An electron paramagnetic resonance (EPR) study on a Y$_{0.992}$Ca$_{0.008}$Ba$_2$Cu$_3$O$_6$: 1 % Gd single crystal with $p_h \approx 0.004$ suggests that in lightly doped Y$_{1-y}$Ca$_y$Ba$_2$Cu$_3$O$_6$, holes localize into an ordered structure.[18] However μSR study of lightly doped YBa$_2$Cu$_3$O$_{6+x}$ ($0 < x < 0.5$) (Ref. 16) suggests that the structural disorder induced by the cation substitution is at the origin of the cluster spin-glass state of the CuO$_2$ plane and, consequently, of the inhomogeneous distribution of the doped holes.

It is well known that the main building blocks of the YBa$_2$Cu$_3$O$_{6+x}$ crystal structure are the Cu(2)O$_2$ planes and Cu(1)O$_x$ chains. The hole doping is achieved by changing the oxygen content in the Cu(1)O$_x$ chains or by heterovalent substitution of some ions in the crystal lattice. The electronic magnetic moments of Cu^{2+}(2) order antiferromagnetically below T_N=420 K, both within the CuO$_2$ plane and between the adjacent planes, with moments aligned in the planes. A single bilayer of CuO$_2$ planes produces a hyperfine magnetic field of about 1 kOe on the Cu(1) site;[19] but in the actual crystal it cancels out due to the symmetric position of Cu(1) with respect to the two neighboring Cu(2) ions pertaining to distinct CuO$_2$ bilayers. So, for the nuclear spins of the nonmagnetic Cu$^+$(1) ion one observes a pure nuclear quadrupole resonance (NQR) spectrum at ν_Q=30.2 MHz for ^{63}Cu at 4.2 K. A consequence of this cancellation of the internal field is that the Cu(1) nucleus is a good probe of what is happening in the planes. One can expect that the disturbance of the antiferromagnetic network by doped holes will inevitably break down this cancellation and influence both spectroscopic and dynamic properties of the Cu(1) nuclear spins. Such an influence was observed for YBa$_2$Cu$_3$O$_{6+x}$ (x

=0.1–0.4) in Ref. 20. Similar effects on Cu(1) nuclei coming from the disturbance in the Cu(2) antiferromagnetic network is expected in $Y_{1-y}Ca_yBa_2Cu_3O_6$ compounds. It should be noticed that $Ca^{2+} \rightarrow Y^{3+}$ substitution does not modify the atomic structure of the Cu(1) plane, so that the electronic structure of this Cu(1) empty chain plane is not modified with respect to that of the parent $YBa_2Cu_3O_6$ compound.

In this paper we report the results of an extensive study of the dynamics of doped holes and their distribution in the CuO_2 plane of the $Y_{1-y}Ca_yBa_2Cu_3O_6$ ($y=0.02$ and 0.04) antiferromagnetic compound. The heterovalent substitution $Ca^{2+} \rightarrow Y^{3+}$ produces $y/2$ holes per unit cell in the CuO_2 plane. Thus, in these samples the hole content is $p_h \approx 0.01$ and 0.02, respectively, quite far from the concentrations $0.05 < p_h < 0.065$, for which superconductivity appears in $Y_{1-y}Ca_yBa_2Cu_3O_6$.[21] The Néel temperature for both samples exceeds 150 K,[4,17] although the Néel transition is rather extended. To compare those doped cases with the situation in the parent compound, we have done studies on two samples $YBa_2Cu_3O_{6.09}$ and $YBa_2Cu_3O_{6.12}:Zn^{2+}:Tm^{3+}$ for which we do not expect any hole doping.

II. EXPERIMENTAL PROCEDURE AND RESULTS

Ceramic samples of $Y_{0.98}Ca_{0.02}Ba_2Cu_3O_{6.016}$ (further referred to as $YBCO_6:Ca2$) and $Y_{0.96}Ca_{0.04}Ba_2Cu_3O_{6.006}$ ($YBCO_6:Ca4$) and a reference powder sample of $YBa_2Cu_3O_{6.09}$ ($YBCO_6$) were prepared by standard solid-state reaction. Also a powder sample of $Tm_{0.05}Y_{0.95}Ba_2(Cu_{0.98}Zn_{0.02})_3O_{6.12}$ ($YBCO_6:Zn,Tm$) in which Zn^{2+} ions substitute for $Cu^{2+}(2)$ ions and Tm^{3+} substitutes for Y^{3+} has been studied. These substitutions being isovalent, they do not modify the Cu(2) plane hole content but produce out-of-plane and in-plane disorders, due to the difference of Y^{3+}-Tm^{3+} and $Cu^{2+}(2)$-Zn^{2+} ionic radii. The oxygen content in both $YBCO_6$ and $YBCO_6:Zn,Tm$ samples is not sufficient to induce a significant hole doping of the CuO_2 plane. So, this set of samples should allow us then to compare the respective influences of structural disorder and hole doping on the spectroscopic and dynamic properties of the chain Cu(1) site. A home-built-pulsed NMR/NQR spectrometer was used for measuring Cu(1) NQR spectra and relaxation.

A. Transverse relaxation rates

The transverse decay curves were obtained by varying the delay τ between the two radio frequency pulses of a standard spin-echo sequence ($\pi/2$-τ-π) allowing to produce a spin echo $A(2\tau)$ at time 2τ. For the transverse relaxation the fitting function used was

$$A(2\tau) = A(0)\exp[-(2\tau/T_2)^{N_2}]. \quad (1)$$

The spin-echo decay curves of Cu(1) nuclei in reference $YBCO_6$ and $YBCO_6:Zn,Tm$ samples could be fitted well by function (1) with $N_2 \geq 1$ in all the temperature range from 4.2 to 300 K. The same fitting with $N_2 \sim 1$ could be done for Ca samples, but only at high temperatures. In both $YBCO_6:Ca$ samples, it is no longer possible to fit the Cu(1) transverse
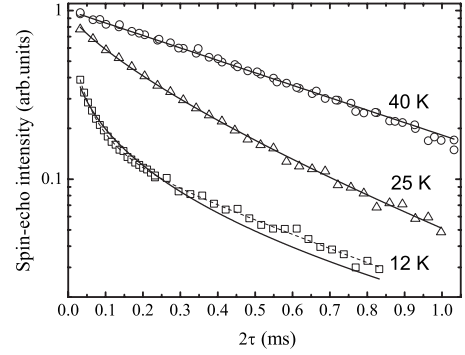

FIG. 1. The Cu(1) echo decay curves in the $YBCO_6:Ca2$ sample at certain temperatures. Solid lines are fitting results by function (1); dashed line is the result of fitting by function (2).

relaxation curve to a single "stretched" exponent (Fig. 1) at low temperatures, as was noticed also in Ref. 20 for $YBa_2Cu_3O_{6+x}$ ($x=0.2$–0.4). Instead, one can analyze the data by assuming that one has two types of copper sites with different nuclear transverse relaxation rates. The best fitting procedure was obtained using function (2) which includes a fraction P of fast relaxing component with a "stretched"-exponential relaxation curve and a long relaxing fraction $1-P$ with a pure exponential relaxation curve,

$$A(2\tau) = A(0)\{P \exp[-(2\tau/T_{21})^{N_2}] + (1-P)\exp(-2\tau/T_{22})\}. \quad (2)$$

The full data set for the transverse relaxation of Cu(1) is shown in Fig. 2. It is clearly seen that the separation of Cu(1) nuclei into fast and slow-relaxing parts could be reliably established by Cu(1) NQR below approximately 20 and 23 K for the $YBCO_6:Ca2$ and $YBCO_6:Ca4$ samples, respectively. The transverse relaxation rate of the fast relaxing Cu(1) goes
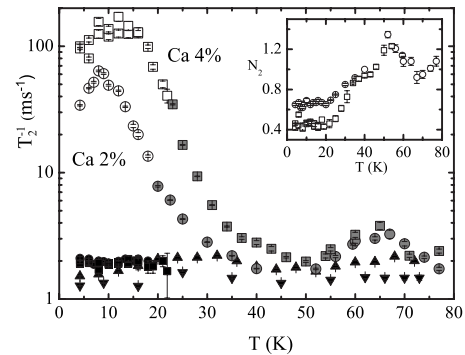

FIG. 2. The temperature dependence of transverse nuclear relaxation rate of $^{63}Cu(1)$ in the samples $YBCO_6:Ca2$ (circles), $YBCO_6:Ca4$ (squares), $YBCO_6$ (black up triangles), and $YBCO_6:Zn,Tm$ (black down triangles). Gray symbols represent the $T_2^{-1}(T)$ obtained from experimental data with fitting function (1), open circles and open squares are $T_2^{-1}(T)$ of short relaxing Cu(1) nuclei obtained with fitting function (2) for $YBCO_6:Ca2$ and $YBCO_6:Ca4$ samples, respectively; black circles and black squares represent $T_2^{-1}(T)$ of slow-relaxing Cu(1) for $YBCO_6:Ca2$ and $YBCO_6:Ca4$ samples. Inset: The T dependence of N_2 [Eqs. (1) and (2)] for $YBCO_6:Ca2$ (circles) and $YBCO_6:Ca4$ (squares) samples.

TABLE I. Part of fast relaxing Cu(1) nuclei (P).

Sample	Temperature				
	1.6 K	4.2 K	8 K	12 K	15 K
$Y_{0.98}Ca_{0.02}Ba_2Cu_3O_{6.016}$	8(3)%	52(5)%	60(4)%		63(4)%
$Y_{0.96}Ca_{0.04}Ba_2Cu_3O_{6.006}$	43(2)%	66(4)%		85(3)%	

through a maximum at 8 and 12 K for YBCO$_6$:Ca2 and YBCO$_6$:Ca4 samples, respectively. The results of careful measurement of the Cu(1) fast relaxing part P at some temperatures are represented in Table I. At the temperatures of the peaks, the fraction P of fast relaxing Cu(1) is maximal and reaches approximately 60% for YBCO$_6$:Ca2 and approximately 85% for YBCO$_6$:Ca4. It decreases then at low temperatures: fitting of the spin-echo decay curves at T =1.6 K gives P=5–10 % and $P \sim 43\%$, respectively. As can be seen in Fig. 2 the value of the relaxation rate for the slow-relaxing copper was found very similar to that in the undoped reference compound, so that the Cu(1) site T_2 is only weakly perturbed by the hole doping. So a substantial fraction of the Cu(1) nuclear spins are totally insensitive to the existence of doped holes.

Also it is clearly seen that at $T \sim 65$ K, there is one more peak in the $1/T_2$ temperature dependence of Cu(1) nuclei in both YBCO$_6$:Ca samples (Fig. 2). In the whole temperature range around 65 K, the echo decay curve could be well fitted to the stretched exponent with N_2 slightly exceeding 1 on both sides of the peak, but within the peak N_2 decreases down to $N_2 \approx 0.9$. It was not possible to separate the echo decay curve into two exponential contributions. This evidences the occurrence of a small distribution of the Cu(1) transverse relaxation rates at the 65 K peak. Similar behavior of the Cu(1) nuclear transverse relaxation at $T \sim 70$ K was found out in slightly doped YBa$_2$Cu$_3$O$_{6+x}$ ($0.1 < x < 0.4$).[20]

B. Spin-lattice relaxation

The spin-lattice (longitudinal) relaxation recovery curves were obtained using the standard three-pulse techniques $(\pi/2)$-t-$(\pi/2$-τ-$\pi)$ where the first $(\pi/2)$ pulse saturates the NQR line, and the spin-echo sequence allows to measure the recovery $A(t)$ of the nuclear magnetization after the evolution time t. In the undoped samples, the magnetization recovery has been found as nonexponential and is well fitted by a stretched exponential,

$$A(t) = A(\infty)\{1 - B \exp[-(t/T_1)^{N_1}]\}. \quad (3)$$

It is known that such a stretched-exponential behavior of the relaxation with $N_1 < 1$ is inherent to the case of a distribution of relaxation rates among the nuclei and that the value of N_1 can be considered as a quantitative measure of the extent of this distribution.

For both lightly doped YBCO$_6$:Ca samples, the shape of the recovery curves changed with temperature and could be also well fitted to a stretched exponent at high temperature, but with a value of N_1 which varies with temperature. At low T, the separation of Cu(1) nuclei into two kinds could be

traced also in the longitudinal relaxation for both YBCO$_6$:Ca samples. At certain temperatures the longitudinal relaxation rates of two kinds of Cu(1) differ from each other so much that it could be easily seen in the shape of the longitudinal magnetization recovery curves (Fig. 3). There the longitudinal relaxation curves were fitted here again by a two component contribution,

$$A(t) = A(\infty)[\{1 - B \exp[-(t/T_{11})^{N_{11}}]\}$$
$$+ C\{1 - B \exp[-(t/T_{12})^{N_{12}}]\}], \quad (4)$$

where T_{11} and T_{12} are longitudinal relaxation times of the two types of Cu(1)'s. Function (4) has several fitting parameters, which limits the reliability of the fits. In order to minimize the number of fitting parameters, we measured the longitudinal relaxation rate of one kind of Cu(1)'s separately. The standard three-pulse sequence was used, but the τ delay between pulses in the spin-echo measuring pair $(\pi/2$-τ-$\pi)$ was taken as long as necessary to get a complete decay of the spin echo of the fast relaxing Cu(1) nuclei. The parameters $1/T_{11}$, N_{11}, and saturation factor B obtained by such a method were put in function (4) as fixed parameters. Also it was found that one kind of Cu(1) nuclei has both fast transverse and fast longitudinal relaxations, respectively, and the other kind of Cu(1)'s has both long T_2 and T_1. Slow relaxing Cu(1) nuclei also have $1/T_1$ and N close to $1/T_1$ and N of Cu(1) in the undoped reference YBCO$_6$ samples. The temperature dependences of the longitudinal relaxation rates of Cu(1) nuclei for all samples are represented in Fig. 4.

Let us note first that—as for $1/T_2$—the spin-lattice relaxation of the fraction of slow-relaxing nuclei, which dominates at high temperature, is the same as that of the pure-undoped YBCO$_6$ sample. This evidences that Cu(1), in these AF phases, is somewhat insensitive to hole doping when
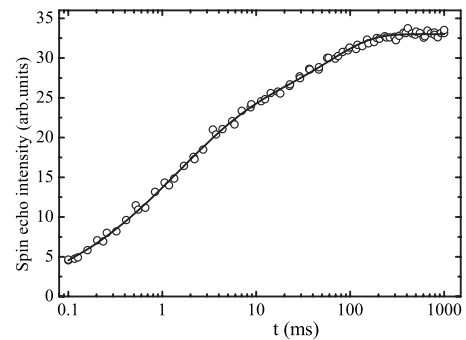

FIG. 3. Longitudinal magnetization recovery curve measured in YBCO$_6$:Ca2 at T=16 K. Solid line is a result of fitting by function (4).
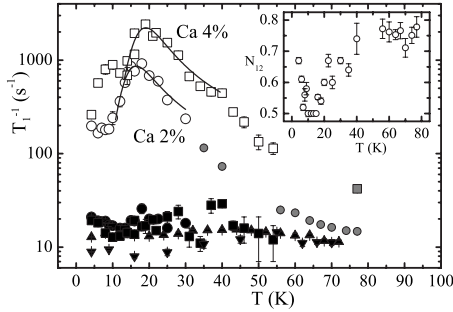
FIG. 4. The temperature dependence of ^{63}Cu(1) longitudinal nuclear relaxation rate in the samples YBCO$_6$:Ca2 (circles), YBCO$_6$:Ca4 (squares), YBCO$_6$ (black up triangles), and YBCO$_6$:Zn,Tm (black down triangles). Gray symbols represent the $T_1^{-1}(T)$ obtained from experimental data with fitting function (3), open circles and open squares are $T_1^{-1}(T)$ of short relaxing Cu(1) nuclei obtained with fitting function (4) for YBCO$_6$:Ca2 and YBCO$_6$:Ca4 samples, respectively; black circles and black squares represent $T_1^{-1}(T)$ of slow-relaxing Cu(1) for YBCO$_6$:Ca2 and YBCO$_6$:Ca4 samples. Solid lines are fitting curves by Eq. (5), for parameters see text. Inset: The T dependence of N_{12} [Eq. (4)] for YBCO$_6$:Ca2 sample. The N_{11} parameter almost did not depend on T and was close to 0.8 (not shown). The dependence for YBCO$_6$:Ca4 sample was similar (not shown).

those are highly delocalized and that the main incidence seen on fast relaxing nuclei occurs when localization of holes takes place. On the contrary the Cu(2) nuclear spins which are coupled through a huge hyperfine coupling ($\sim$10 T/μB_{micro}) to the doped Cu^{2+} electron spins are highly affected by hole doping.[22] Let us note that the T_1 (as T_2) of the pure compound is again surprisingly found temperature independent, which is somewhat unexpected and reflects that the magnon contribution to the relaxation is not important. Finally, as for $1/T_2$, the spin-lattice relaxation is not modified in YBCO$_6$:Zn,Tm samples with respect to that of YBCO$_6$, as can be seen in Figs. 2 and 4. This reveals that the associated magnetic disorder for Zn or structural disorder for Tm does not affect the spin dynamics of the Cu(1) site. At this stage we do not understand then the actual origin of this remarkable T-independent spin dynamics detected by the Cu(1) nuclear spin in the parent compounds.

In YBCO$_6$:Ca samples $1/T_1$ of the short relaxing Cu(1) has a peak at temperatures of 16 and 19 K for YBCO$_6$:Ca2 and YBCO$_6$:Ca4, respectively. The two types of Cu(1) could be distinguished in longitudinal relaxation for $T < 30$ K and $T < 55$ K, respectively, for the two samples.

C. NQR spectra

The large difference between the relaxation rates of the two kinds of Cu(1)'s gives a chance to measure their NQR spectra separately and to trace the evolution of the NQR lines with temperature. The following method was used (Fig. 5):

(1) The NQR spectrum of slow-relaxing Cu(1)'s was measured by the ($\pi/2$-τ-π) sequence with long delay time τ_1.

(2) The full NQR spectrum of both kinds of Cu(1) nuclei was measured by the ($\pi/2$-τ-π) sequence with short delay time τ_2.
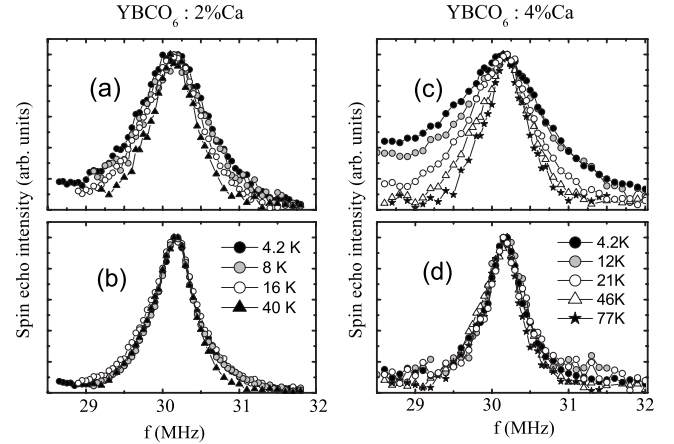

FIG. 5. ^{63}Cu(1) NQR spectra in YBCO$_6$:Ca2 and YBCO$_6$:Ca4 samples at few temperatures. The spectra of panels (b) and (d) were measured at long delay time $\tau = 150$ μs, thus representing only slow-relaxing Cu(1). The spectra of panels (a) and (c) were measured at short delay time $\tau = 18$ μs and contain both spectra of short and long relaxing Cu(1).

(3) The NQR spectrum of short relaxing Cu(1) nuclei was obtained by subtracting from the full NQR spectrum that of the slow-relaxing Cu(1) spectrum rescaled in intensity to the short delay time τ_2.

The temperature dependences of linewidths of the two types of Cu(1) nuclei are represented in Fig. 6 for both YBCO$_6$:Ca samples. The separation of the Cu(1) NQR spectrum into two contributions was observed at low temperatures. The broad (narrow) lines result from fast (slow) relaxing Cu(1) nuclei, respectively. The linewidth of the narrow NQR line does not depend on temperature down to $\sim$8 and $\sim$4 K in YBCO$_6$:Ca2 and YBCO$_6$:Ca4, respectively, and broadens then at lower T. However the same broadening effect was also observed in the reference-undoped samples at low temperatures. The width of the broad line increases continuously with decreasing T.

III. DISCUSSION

Let us consider now the indications concerning the dynamics and distribution of holes in the CuO$_2$ plane of slightly doped Y$_{1-y}$Ca$_y$Ba$_2$Cu$_3$O$_6$ compounds which can be deduced from this ensemble of experimental results. Let us first com-
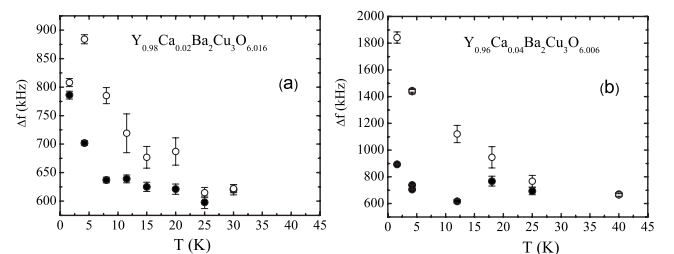
FIG. 6. Temperature dependence of ^{63}Cu(1) NQR linewidths: (a) for YBCO$_6$:Ca2 and (b) for YBCO$_6$:Ca4. Open circles are the widths of the fast relaxing ^{63}Cu(1) line and the solid circles are the widths of the slow-relaxing ^{63}Cu(1) line.

pare with existing data in similar systems to try to single out the physical phenomenon which drives the observed variation in Cu(1) nuclear-spin dynamics.

A. High-temperature data and hole dynamics

The ^{139}La NQR data obtained in undoped La_2CuO_4 compound with spinless Zn^{2+} impurities which substitute the plane Cu^{2+} ions showed a peak in the temperature dependence of $1/T_1$ at temperatures of about 70–100 K.[23] The authors suggest that this modification of the longitudinal relaxation rate can be driven by fluctuations of local moments induced by spinless impurities. In the present work, we have also studied an undoped $YBCO_6:Zn,Tm$ compound, where a small part (2%) of the Cu(2) plane ions was substituted by isovalent Zn^{2+} spinless impurity and 5% of Y^{3+} were substituted by isovalent Tm^{3+}. Due to the different ionic radii, such substitutions still create some disorder in the YBCO structure. This disorder indeed broadens the Cu(1) NQR lines, so that the linewidth in $YBCO_6:Zn,Tm$ sample is similar to that in the $YBCO_6:Ca2:Ca2$ sample. However, no modification of the longitudinal and transverse relaxation rates of Cu(1) nuclei was found at low temperatures. Thus the peaks in the Cu(1) relaxation rates observed in $YBCO_6:Ca$ *are not driven by the disorder introduced by impurities*.

We rather conclude that it is *the slowing down of the doped holes motion* that gives rise to slow magnetic fluctuations on the Cu(1) sites and results in the enhancement of the longitudinal and transverse relaxations of Cu(1) nuclei at low temperatures. This is supported by the fact that a similar behavior of the chain copper relaxation is observed in other lightly doped YBCO cuprates: $YBa_2Cu_3O_{6+x}$ $(0.1 < x < 0.4)$.[20]

Further, as was mentioned above, the nuclear transverse relaxation rate of Cu(1) in $YBCO_6:Ca$ samples displays one more peak at $T \sim 65$ K. This peak was also observed in hole-doped YBCO compounds[20,24] but was not found neither in our undoped $YBCO_6$ nor in undoped $YBCO_6:Zn,Tm$. This also allows us to suggest again that the 65 K peak in $1/T_2$ is due to mobile holes behavior and not due to the disorder. As this enhancement of $1/T_2$ applies at $T \sim 65-70$ K for of *all* Cu(1) nuclei in these hole-doped samples, this is an indication that the holes move freely in the CuO_2 plane at high T and that the motion of the whole assembly of holes slows down at about 65 K; this effect being rather similar for Ca concentrations of 2% and 4%.

It is natural then to search for some peculiarities in transport properties of slightly doped samples. Charge transport measurements in slightly doped $YBa_2Cu_3O_{6+x}$ ($x=0.23$, 0.30, and 0.32) (Refs. 25 and 26) demonstrated that in high-quality single crystals, the in-plane resistivity shows a metallic behavior at temperatures above $\sim 60-70$ K. At low temperatures the resistivity shows insulating temperature evolution that is consistent with a variable-range-hopping behavior of charge carriers. Similar results were obtained in slightly doped $La_{2-x}Sr_xCuO_4$ compounds, but the metallic behavior of the in-plane resistivity was found at temperatures depending on doping level: from $T > 90$ K at $x=0.03$ to $T > 150$ K at $x=0.01$.[27] The magnitude of doped holes mobil-

ity at room temperature is close to that of typical metals in both $YBCO_{6+x}$ and $La_{2-x}Sr_xCuO_4$ (LSCO) compounds.[27] Thus, transport data also suggest that doped holes are distributed homogeneously and move freely in the CuO_2 plane at high temperatures. The observed peak in the transverse relaxation rate at $T \sim 65$ K should then be related with the decrease in hole mobility associated with the evolution of the hole transport behavior from metallic to variable-range hopping.

B. Low-T magnetic state

It is well known that the nuclei probing the planar Cu(2) sites display enhanced T_1 rates at temperatures close to the transition of the CuO_2 plane into a disordered magnetic state inherent to slightly doped HTSCs (Ref. 1) (often denominated shortly as "spin glass," but which is not secured as such). The peak in the $T_1^{-1}(T)$ of fast relaxing Cu(1) is apparently also connected to this transition. The accuracy of our fast relaxing copper T_1^{-1} measurements was not enough to decide whether the relaxation is produced by fluctuating magnetic or electric field, but T_2^{-1} of fast relaxing ^{65}Cu(1) at the peak temperature was larger than that for ^{63}Cu(1). Since the gyromagnetic ratio γ for ^{65}Cu is larger than for ^{63}Cu, contrary to the quadrupole moments, this indicates the magnetic origin of the relaxation. The slowing down of the doped holes motion in the plane at decreasing T also slows down the fluctuations of the magnetic field produced by frustrated Cu(2) electronic magnetic moments located near the doped hole.

According to the Bloembergen-Purcell-Pound theory,[28] the longitudinal relaxation rate caused by the fluctuating magnetic field with an exponential form of correlation function depends on the mean-square amplitude H_1 and correlation time τ_c of fluctuations as follows:

$$\frac{1}{T_1} = \frac{\gamma^2 H_1^2 \tau_c}{1 + \omega_{NQR}^2 \tau_c^2}, \quad (5)$$

with ω_{NQR}—the NQR frequency. The peak in longitudinal relaxation rate appears then when the fluctuations become slow enough to reach the Cu(1) NQR frequency 3×10^7 Hz. As for the enhancement of the transverse relaxation rate, it only occurs when the rate of magnetic fluctuations becomes as low as the pure sample $(T_2)^{-1}$ on the order of tens of kilohertz.[29] All this explains then coherently the appearance of the peak in the transverse relaxation rate of the short relaxing Cu(1) at lower temperatures. Evidently, at even lower temperatures the relaxation rate decreases again when the fluctuations become very slow. Assuming the Arrhenius law for the temperature dependence of $\tau_c(T) = \tau_c(\infty)\exp(\Delta E/T)$ and analyzing $T_1^{-1}(T)$ along the lines of Ref. 29, we get $\Delta E=63(7)$ and 83(9) K, $\tau_c(\infty)=1.2(5) \times 10^{-10}$ and $7(3) \times 10^{-11}$ s, and $H_1=80(3)$ and 130(5) Oe for $YBCO_6:Ca2$ and $YBCO_6:Ca4$ samples, respectively (Fig. 4).

The enhancement of the nuclear longitudinal relaxation rate is produced by the fluctuations of magnetic field perpendicular to the quantization axis of the nuclear-spin system.[30] On the contrary, the enhancement of transverse relaxation
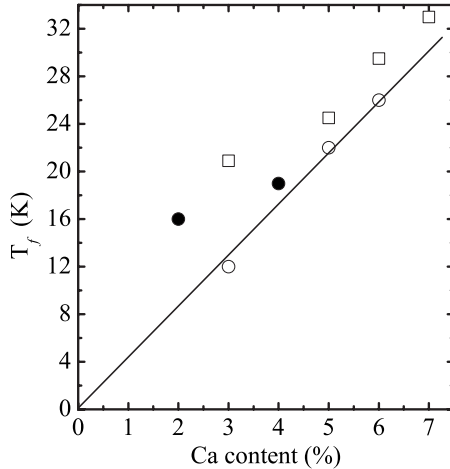
FIG. 7. Doping dependence of the disordered magnetic state temperature T_f in YBCO6: Ca. Open circles and squares are results of μSR experiments represented in Refs. 4 and 31, respectively; solid circles are results obtained from our ^{63}Cu(1) NQR experiments.

rate is produced mainly by the low-frequency fluctuations parallel to the quantization axis.[30] In YBCO$_6$:Ca in the absence of external magnetic field, the quantization axis for the nuclear spins of the twofold-coordinated Cu(1) coincides with the principal axis of the axially symmetric tensor of electric-field gradient and is parallel to the crystallographic c axis. The existence of peaks for both longitudinal and transverse relaxation rates indicates that the fluctuating magnetic fields have components both perpendicular and parallel to the c axis. Apparently the latter appears due to the out-of-plane components of the electronic magnetic moments of Cu(2)$^{2+}$ located near the doped hole.[1–3] The freezing of these spin degrees of freedom in the slightly doped La$_{2-x}$Sr$_x$CuO$_4$ ($x<0.02$) (Ref. 1) and Y$_{1-y}$Ca$_y$Ba$_2$Cu$_3$O$_6$ ($y<0.07$) (Ref. 4) at T_f gives rise to the transition of the plane Cu^{2+} spin system into the disordered magnetic state which is superimposed on the pre-existing AF long-range order at $T<T_f$.

The temperature at which the characteristic time of the magnetic fluctuations slows down to reach the typical frequency of the experimental technique is slightly less in YBCO$_6$:Ca2 ($p_h=0.01$) than in YBCO$_6$:Ca4 ($p_h=0.02$): respectively, 16 and 19 K [peaks in Cu(1) longitudinal relaxation] and 8 and 12 K (peaks in transverse relaxation). These data are compared in Fig. 6 with the temperature T_f of the disordered magnetic state formation obtained by different measurements. They are consistent within experimental accuracy with the results for YBa$_2$Cu$_3$O$_6$:Ca reported in Ref. 31 (Fig. 7). However they do not scale linearly with hole doping as observed in some studies: in Sr-doped La$_{2-x}$Sr$_x$CuO$_4$ (Ref. 1), Li-doped La$_2$Cu$_{1-y}$Li$_y$O$_4$ (Ref. 32), and YBa$_2$Cu$_3$O$_6$:Ca (Ref. 4) compounds. Such linear behavior has been explained theoretically in Ref. 2 if the freezing transverse degrees of freedom are associated with the many-Skyrmion spin texture produced by randomly distributed defects.

C. Distribution of the holes

The inhomogeneous distribution of relaxation observed at low T in the YBCO$_6$:Ca samples reveals a localization of the

doped holes. The impurity ions likely play an important role in this inhomogeneous distribution of the holes and in the emergence of spin-glass behavior, as it takes place, for example, in La$_{2-x}$Sr$_x$CuO$_4$, where part of trivalent La^{3+} is replaced by divalent Sr^{2+}.[2,14] It is natural then to assume that the Ca^{2+} ions, which are out-of-plane centers of electrostatic attraction for the holes, are the relevant pinning centers for the doped holes. Therefore at low T one can expect that the motion of the doped holes is localized in the vicinity of the Ca^{2+} sites, so that the fraction P of fast relaxing Cu(1) nuclei, which sense the slow magnetic fluctuations induced by slow motion of the doped holes in the CuO$_2$ plane, is a measure of the spatial extent of the regions with localized holes. The fraction $1-P$ of other Cu(1) (see Table I) relaxes as Cu(1) in hole-free YBCO$_6$ which points out that they are far enough from the regions where holes localize. The incidence of slow magnetic fluctuations due to the holes on such sites is too small to shortcut the relaxation which prevails in the pure material.

A simple all or nothing model could be used then to determine the fraction of the area S of the CuO$_2$ plane occupied by the localized holes from the NQR in our YBCO$_6$:Ca samples. If we assume that the motions of the holes are correlated in the two adjacent CuO$_2$ planes then S is merely the part P of short relaxing Cu(1) nuclei, i.e., ~63% and ~85%, at the temperature of the $1/T_2$ peaks for the YBCO$_6$:Ca2 and YBCO$_6$:Ca4 samples, respectively.

If the motions of the holes in two adjacent planes are not correlated then $S\approx 1-\sqrt{1-P}$. In this case we obtain S ~40% and ~60%, respectively, for the two samples. In both cases, the area occupied by the doped holes increases with hole doping. However, the size of the regions cannot be directly obtained from our NQR experimental data and requires at least some further analysis.

We estimated the size of the regions by using a simple model in which the doped holes regions formed around Ca^{2+} impurities are disks in the CuO$_2$ plane. Square samples (100$\times$100 lattice constants) of the CuO$_2$ plane were considered, with the Ca impurities positioned at random for the two considered concentrations. The disk diameter was increased until the total fractional area occupied by the disks reached *for both samples* the experimental values of S obtained from NQR as explained here above. At the temperature of the $1/T_2$ peaks, we obtained then estimates of ~6 and ~4 lattice constants for the radius of the disks depending whether we assume that the motions of the holes are correlated or uncorrelated.

If we pursue such an analysis to temperatures smaller than that of the $1/T_2$ and $1/T_1$ peaks, we would conclude that the size of the doped hole region is reduced with decreasing T (see Table I). This could be due to the bonding of the doped holes with the Ca^{2+} impurity, as the Ca^{2+} ion in the Y^{3+} site is a center of electrostatic attraction for the holes. The slowing down of the magnetic fluctuations on the Cu(1) site indeed gives rise to a decrease in the transverse relaxation rate at temperatures lower than those of the $1/T_2$ peaks. One expects that at temperatures much smaller than T_f, the doped holes become completely frozen on fixed orbitals around the Ca^{2+}. The area S should reach then a value which increases initially linearly with hole content. However, the relaxation

rates become so small in this experimental range that we cannot distinguish then so reliably the slow from the fast relaxation regime.

IV. CONCLUSION

In conclusion, our Cu(1) NQR study in slightly doped YBCO$_6$:Ca compounds showed that the doped holes are distributed homogeneously in the CuO$_2$ plane at high temperatures and move freely in the plane. At about 65 K a decrease in hole mobility is observed and is associated with the evo-lution of the hole transport behavior from metallic to variable-range hopping. The doped hole motion slows down with decreasing temperature and the holes localize in re-stricted regions. We suggest that the out-of-plane Ca^{2+} impu-rity serves as pinning center for the doped holes. At the tem-perature of $1/T_2$ peaks the radius of the regions occupied by holes is estimated as 4–6 lattice constants around the impu-rity ions. As a whole, these regions occupy then 40–60 % of the CuO$_2$ plane. For the time being, we could not achieve enough sensitivity to detect the ultimate size of the orbits on which the holes freeze around the Ca^{2+} ions at temperatures much lower than that of the $1/T_2$ peaks.

[1] F. C. Chou, F. Borsa, J. H. Cho, D. C. Johnston, A. Lascialfari, D. R. Torgeson, and J. Ziolo, Phys. Rev. Lett. **71**, 2323 (1993).

[2] R. J. Gooding, N. M. Salem, and A. Mailhot, Phys. Rev. B **49**, 6067 (1994).

[3] F. Borsa, P. Carretta, J. H. Cho, F. C. Chou, Q. Hu, D. C. Johnston, A. Lascialfari, D. R. Torgeson, R. J. Gooding, N. M. Salem, and K. J. E. Vos, Phys. Rev. B **52**, 7334 (1995).

[4] Ch. Niedermayer, C. Bernhard, T. Blasius, A. Golnik, A. Mood-enbaugh, and J. I. Budnick, Phys. Rev. Lett. **80**, 3843 (1998).

[5] C. Panagopoulos, B. D. Rainford, J. R. Cooper, and C. A. Scott, Physica C **341**, 843 (2000).

[6] M.-H. Julien, Physica B **329**, 693 (2003).

[7] S. A. Kivelson and V. J. Emery, in *Stripes and Related Phenom-ena*, edited by A. Bianconi and N. L. Saini, Selected Topics in Superconductivity Vol. 8, Part 2 (Springer, New York, 2002), pp. 91–100; V. J. Emery, S. A. Kivelson, and J. M. Tranquada, Proc. Natl. Acad. Sci. U.S.A. **96**, 8814 (1999).

[8] J. M. Tranquada, B. J. Sternlieb, J. D. Axe, Y. Nakamura, and S. Uchida, Nature (London) **375**, 561 (1995).

[9] M. Matsuda, M. Fujita, K. Yamada, R. J. Birgeneau, Y. Endoh, and G. Shirane, Phys. Rev. B **65**, 134515 (2002).

[10] L. P. Pryadko, S. A. Kivelson, and D. W. Hone, Phys. Rev. Lett. **80**, 5651 (1998).

[11] A. Paolone, F. Cordero, R. Cantelli, and M. Ferretti, Phys. Rev. B **66**, 094503 (2002).

[12] M. Bosch and Z. Nussinov, arXiv:cond-mat/0208383 (unpub-lished).

[13] A. Aharony, R. J. Birgeneau, A. Coniglio, M. A. Kastner, and H. E. Stanley, Phys. Rev. Lett. **60**, 1330 (1988).

[14] R. J. Gooding, N. M. Salem, R. J. Birgeneau, and F. C. Chou, Phys. Rev. B **55**, 6360 (1997).

[15] H. Alloul, J. Bobroff, M. Gabay, and P. J. Hirschfeld, arXiv:0711.0877 (unpublished).

[16] S. Sanna, G. Allodi, G. Concas, and R. De Renzi, J. Supercond. **18**, 169 (2006).

[17] H. Casalta, H. Alloul, and J.-F. Marucco, Physica C **204**, 331 (1993).

[18] A. Janossy, T. Feher, and A. Erb, Phys. Rev. Lett. **91**, 177001 (2003).

[19] A. V. Dooglav, H. Alloul, M. V. Eremin, and A. G. Volodin, Physica C **272**, 242 (1996).

[20] M. Matsumura, H. Yamagata, and Y. Yamada, J. Phys. Soc. Jpn. **58**, 805 (1989).

[21] J. L. Tallon, C. Bernhard, H. Shaked, R. L. Hitterman, and J. D. Jorgensen, Phys. Rev. B **51**, 12911 (1995).

[22] P. Mendels, H. Alloul, J. F. Marucco, J. Arabski, and G. Collin, Physica C **171**, 429 (1990).

[23] M. Corti, A. Rigamonti, F. Tabak, P. Carretta, F. Licci, and L. Raffo, Phys. Rev. B **52**, 4226 (1995).

[24] We have checked this point ourselves as well in a YBCO$_{6.25}$ sample.

[25] Y. Wang and N. P. Ong, Proc. Natl. Acad. Sci. U.S.A. **98**, 11091 (2001).

[26] Y. Ando, A. N. Lavrov, and K. Segawa, Phys. Rev. Lett. **83**, 2813 (1999).

[27] Y. Ando, A. N. Lavrov, S. Komiya, K. Segawa, and X. F. Sun, Phys. Rev. Lett. **87**, 017001 (2001).

[28] N. Bloembergen, E. M. Purcell, and R. V. Pound, Phys. Rev. **73**, 679 (1948).

[29] S. Fujiyama, M. Takigawa, and S. Horii, Phys. Rev. Lett. **90**, 147004 (2003); M. Takigawa and G. Saito, J. Phys. Soc. Jpn. **55**, 1233 (1986).

[30] C. P. Slichter, *Principles of Magnetic Resonance* (Springer-Verlag, New York, 1990).

[31] C. E. Stronach, D. K. Noakes, X. Wan, Ch. Niedermayer, C. Bernhard, and E. J. Ansaldo, Physica C **311**, 19 (1999).

[32] T. Sasagawa, P. K. Mang, O. P. Vajk, A. Kapitulnik, and M. Greven, Phys. Rev. B **66**, 184512 (2002).